201026020A

厚生労働科学研究費補助金

認知症対策総合研究事業

アルツハイマー病の新規細胞医薬開発に関する臨床応用研究

平成22年度　総括研究報告書

研究代表者　内村　健治

平成23（2011）年　3月

別紙２

目　　次

別紙3

厚生労働科学研究費補助金（認知症対策総合研究事業）
総括研究報告書

アルツハイマー病の新規細胞医薬開発に関する臨床応用研究

研究代表者　内村　健治　　独立行政法人　国立長寿医療研究センター　室長

研究要旨：　骨髄由来ミクログリア細胞がアルツハイマー病（AD）病態に伴って脳内へ移行し、神経毒性アミロイドβタンパク（Aβ）を積極的に除去していることがモデルマウスを使用した解析より国内外で明らかになってきた。アルツハイマー病脳内細胞浸潤に細胞表面分子セレクチンおよびその認識糖鎖が深く関わる事を申請者は以前明らかにした。モデルマウスの結果が実際にヒトAD発症においても観察されるか否かを明らかにするため、ヒトミクログリア細胞およびAD剖検脳における当該分子の発現を検証した。すなわち、本申請研究はADモデルマウスで得られた知見および結果をヒト臨床サンプルの使用による臨床研究へ応用するために立案された。本申請研究は脳移行性細胞を利用した細胞医薬によりこの問題を解決し、AD新規治療法開発の技術基盤を提供することを目的とする。本研究一年目にはヒト骨髄由来細胞株を入手しその細胞表面における分子の発現を検証した。その結果、セレクチン認識糖鎖が発現していることを確認した。AD病態脳における当該細胞の動態を生体内ビデオ蛍光顕微鏡技術で解析することを継続している。一方、医療法人さわらび会福祉村病院 赤津裕康研究協力者より提供された非認知症８例、AD８例のヒト剖検脳サンプルにおけるセレクチンおよびリガンド糖鎖の発現変動を解析した。ヒト試料を用いた研究実施に際しては人権の保護および個人情報の保護に最大限の注意を払うことを理解遵守した。AD剖検脳嗅内皮質におけるセレクチン分子の発現上昇をウェスタンブロット法により一部明らかにした。また、認知機能の中枢である海馬においてリガンド糖鎖合成酵素のAD群における特異的発現上昇を確認した。これらの結果はADモデルマウスで観察された骨髄由来ミクログリア細胞がAD病態に伴って脳内へ移行するという現象がヒトADでも起きている可能性を示唆した。AD細胞医薬開発の技術基盤の提供が強く期待された。

A．研究目的

骨髄単球由来ミクログリアがアルツハイマー病（AD）の病態に伴い脳内に浸潤することがモデルマウスを用いた解析により報告されている（Simard et al., Neuron, 2006; El Khoury et al., Nat Med 2007など）。脳内へ移行した骨髄由来ミクログリア細胞は神経毒性アミロイドβタンパク（Aβ）を積極的に除去していることが国内外で明らかになってきた。しかしながらその脳内移行のメカニズムは不明である。申請者は以前、末梢投与マウスミクログリア細胞の脳内動態を生体内ビデオ蛍光顕微鏡によりイメージング解析することに成功した。すなわち、当該脳移行性細胞の脳内浸潤におけるセレクチン-糖鎖の分子メカニズムの重要性をADモデルマウスにより明らかにした。本申請研究はADモデルマウスで得ら

れた知見および結果をヒト臨床サンプルの使用による臨床研究へ応用するために立案された。AD治療法開発における問題の一つは遺伝子等の効率的な脳内動員法が確立していないことである。本申請研究は脳移行性細胞を利用した細胞医薬によりこの問題を解決し、AD新規治療法開発の技術基盤を提供することを目的とする。

B．研究方法

申請者は生体内ビデオ蛍光顕微鏡を本研究室に設置し末梢投与マウスミクログリア細胞のADモデルマウス脳内におけるローリングおよび接着のイメージング解析に成功した。本研究１年目はこの成果をヒトミクログリア細胞へ応用した。ヒトミクログリア細胞は市販のヒト細胞株U937を用いた。U937におけるセレクチン認識糖鎖の発現をフローサイトメトリーにより確認した。アルツハイマー病および非認知症対照群でそれぞれ８例の剖検脳凍結サンプル（海馬および嗅内皮質）の提供を受けた。セレクチンおよびリガンド糖鎖の発現をウェスタンブロット法により解析した。我々のADモデルマウスの結果ではE-セレクチンの発現誘導が観察されているのでヒト剖検脳においてもE-セレクチンを重点的に検証した。また、セレクチンが認識するシアリルルイスX様糖鎖リガンドの発現も同様に解析した。実験解析の実施はすべて国立長寿医療研究センターとし、徹底した倫理審査の承認のもとで行った。医療法人さわらび会福祉村病院で死亡し病理解剖を行った症例の中で、採取サンプルの研究目的の使用に承諾が得られた剖検試料を解析した。

（倫理面への配慮）

研究実施に先立ち、各研究実施協力機関の倫理委員会による厳正中立な審査を受け、研究実施計画の承認を受ける。特にヒト試料を用いた研究実施に際しては人権の保護および個人情報の保護に最大限の注意を払うことを理解遵守し一層の徹底を図る。また、1）インフォームドコンセントの徹底、2）検体の使用及び保存についての中止請求を含む研究協力同意書の十分な説明、3）検体保存責任者を設置し当該者以外には連結不可能な匿名化を施したうえでのサンプル及びデータの保管、さらにスタンドアローンのコンピューターを用いたデータ処理、鍵のかかるキャビネット内へのデータ保管を行う。 本研究において遺伝子の抽出・保管および遺伝子発現の解析は行わず、遺伝情報に触れる事はない。

研究実施に先立ち、研究実施機関である国立長寿医療センターの倫理委員会による厳正中立な審査を受け、研究実施計画の承認を受けた。本申請研究で実施するモデルマウス対象研究はすべて本センター設置の遺伝子組換え生物実験安全委員会の審査を受け承認を得た。また、本センター設置の実験動物委員会および動物実験倫理委員会の審査を受け承認を得た。本研究課題に参画する者は「遺伝子組換え生物等の使用等の規制による生物の多様性の確保に関する法律（カルタヘナ法）」、「動物の愛護及び管理に関する法律」および「動物を用いる生物医学研究のための国際指導原則」の更なる理解を確認し遵守した。

C．研究結果

ヒトミクログリア細胞株U937においてセレクチン認識糖鎖の細胞表面発現を確認した。引き続きAD病態脳における当該細胞の動態を生体内ビデオ蛍光顕微鏡技術で解析する。一方、医療法人さわらび会福祉村病院 赤津裕康研究協力者より提供された非認知症８例、AD８例のヒト剖検脳サンプルにおけるセレクチンおよびリガンド糖鎖の発現変動を解析した。AD剖検脳嗅内皮質におけるセレクチン分子の発現上昇をウェスタンブロット法により一部明らかにした。認知機能の中枢である海馬においてセレクチンリガンド糖鎖の発現を検証したが困難

であったため、リガンド糖鎖合成酵素の発現を検証した。AD群においてセレクチンリガンド糖鎖合成酵素の一種が特異的に発現上昇を示すことを明らかにした。ヒトサンプルの採取はすべて医療法人さわらび会福祉村病院で行ったものを用いた。ヒトサンプルの解析はすべて国立長寿医療研究センター 研究所で行った。

D．考察

AD嗅内皮質におけるセレクチンの発現上昇は、ADモデルマウスで観察された骨髄由来ミクログリア細胞がAD病態に伴って脳内へ移行するという現象がヒトでも起きている可能性を強く示唆した。セレクチンの発現は炎症性サイトカインにより制御されている。この事から，AD脳における細胞浸潤が末梢炎症時における炎症局所への細胞浸潤と一部メカニズムを共有している可能性が示唆された。また、ある種のセレクチン糖鎖合成酵素の発現増加はこれらの可能性を強く支持するものであった。

E．結論

アルツハイマー病の病態に伴う骨髄由来ミクログリア細胞の脳内移行がヒトAD脳でも起きている可能性が示された。セレクチン糖鎖合成酵素の発現がAD脳で特異的に増加している。本研究で得られた知見および結果を今後さらにスケール拡大した臨床研究へ発展させることが強く望まれた。

F.健康危険情報

該当なし。

G．研究発表

1．論文発表

Hossain MM, Hosono-Fukao T, Tang R, Hosono-Fukao, T., Ohtake-Niimi, S., Nishitsuji, K., Hossain, M. M., van Kuppevelt, T. H., Michikawa, M. and Uchimura, K. RB4CD12 epitope expression and heparan sulfate disaccharide composition in brain vasculature.
J. Neurosci. Res., in press

Nishitsuji, K., Hosono, T., Uchimura, K. and Michikawa, M. Lipoprotein lipase is a novel Abeta- binding protein that promotes glycosaminoglycan-dependent cellular uptake of Abeta in astrocytes.
J. Biol. Chem., 286:6393-6401, 2011

内村健治 細胞外スルファターゼSulfによるヘパラン硫酸糖鎖機能の調節 *生化学* 83: 216-223, 2011

2．学会発表

Hosono T, Hossain M, Britschgi M, Akatsu H, van Kuppevelt T, Michikawa M, Wyss-Coray T, Uchimura K.
The Sulf-degrading heparan sulfate epitope accumulates in cerebral amyloid ß plaques of mouse models and patients of Alzheimer's disease
25th International Carbohydrate Symposium (ICS2010) Makuhari Messe, Makuhari, Aug, 2, 2010

Hossain M, Hosono T, Niimi S, van Kuppevelt T, Michikawa M, Rosen S, Uchimura K.
Immunolocalization of the RB4CD12 anti-heparan sulfate epitope in the brain and its degradation by Sulfs, extracellular endosulfatases
25th International Carbohydrate Symposium (ICS2010) Makuhari Messe, Makuhari, Aug, 5, 2010

内村健治
セレクチン認識および血管外細胞遊走に関

わる糖鎖関連酵素
-骨髄由来細胞のアルツハイマー病脳内浸潤-
第４回ミッドカイン研究会　名古屋大学医学部　2010年8月9日、名古屋

内村健治
アルツハイマー病モデルマウス脳内に発現されるケラタン硫酸糖鎖の解析
第１回加藤記念バイオサイエンス研究振興財団研究発表会 2010年10月22日、東京

細野友美、新美しおり、モタラブホサイン、マーカスブリッチギ、赤津裕康、菅谷典子、木全弘治，道川誠、トニーワイスコレイ，内村健治
アルツハイマー病モデルマウス脳内に発現するヘパラン硫酸糖鎖の内部ドメイン構造の解析　第29回日本認知症学会　2010年11月5日、名古屋

Fukao-Hosono T, Hossain M, Ohtake-Niimi S , van Kuppevelt T , Michikawa M, Rosen S and Uchimura K Immunolocalization of the RB4CD12 Anti-Heparan Sulfate Epitope in Brain Microvessels and Its Degradation by Sulf-1 and Sulf-2 Annual meeting of Glycobiology 2010, St. Pete Beach, USA, Nov 8, 2010

細野友美、新美しおり、ホサインモタラブ、菅谷典子、赤津裕康、トニーワイスコレイ、木全弘治、道川誠、内村健治
アルツハイマー病モデルマウス大脳皮質に発現するヘパラン硫酸グリコサミノグリカンの構造解析　第83回日本生化学会大会
2010年12月9日、神戸

Kenji Uchimura
Selectin-carbohydrates interaction in extravasation of bone marrow-derived cells into Alzheimer brain
Wyss-Coray Lab Seminar, Stanford University, 2/14/2011, Palo Alto

H. 知的財産権の出願・登録状況（予定を含む。）
１．特許取得
なし

２．実用新案登録
なし

３．その他
なし

別紙４

研究成果の刊行に関する一覧表

雑誌

発表者氏名	論文タイトル名	発表誌名	巻号	ページ	出版年
Hosono-Fukao, T., Ohtake-Niimi, S., Nishitsuji, K., Hossain, M. M., van Kuppevelt, T. H., Michikawa, M. and Uchimura, K.	RB4CD12 epitope expression and heparan sulfate disaccharide composition in brain vasculature.	*J. Neurosci. Res.*	in press	in press	in press
Nishitsuji, K., Hosono, T., Uchimura, K. and Michikawa, M	Lipoprotein lipase is a novel Abeta- binding protein that promotes glycosaminoglycan-dependent cellular uptake of Abeta in astrocytes.	*J. Biol. Chem.*	286	6393-6401	2011
内村健治	細胞外スルファターゼSulfによるヘパラン硫酸糖鎖機能の調節	生化学	86	216-223	2011

研究成果の刊行物・別刷

RB4CD12 epitope expression and heparan sulfate disaccharide composition in brain vasculature

Tomomi Hosono-Fukao[1], Shiori Ohtake-Niimi[1], Kazuchika Nishitsuji[2], Md. Motarab Hossain[1], Toin H. van Kuppevelt[3], Makoto Michikawa[2], and Kenji Uchimura[1,2]

[1]Section of Pathophysiology and Neurobiology, [2]Department of Alzheimer's Disease Research, National Center for Geriatrics and Gerontology, Japan
[3]Department of Biochemistry 280, Nijmegen Centre for Molecular Life Sciences, Radboud University Nijmegen Medical Center, The Netherlands

Running Title: RB4CD12 anti-HS epitope in brain vessels

Address correspondence to: Kenji Uchimura, Section of Pathophysiology and Neurobiology, Department of Alzheimer's Disease Research, National Center for Geriatrics and Gerontology
35 Gengo, Morioka, Obu, Aichi 474-8511, Japan
Phone: +81-562-46-2311, Fax: +81-562-46-3157, e-mail: arumihcu@ncgg.go.jp

This work was supported by Japanese Health and Labour Sciences Research Grants [Comprehensive Research on Aging and Health H19-001 and H22-007 to K.U.], a Grant-in-Aid from the Ministry of Education, Science, Sports, Culture [22790303 to K.U.] and in parts by the Takeda Science Foundation [to K.U.], the Kato Memorial Bioscience Foundation [to K.U.], and the Uehara Memorial Foundation [to K.U.].

ABSTRACT

RB4CD12 is a phage display antibody that recognizes a heparan sulfate (HS) glycosaminoglycan epitope. The epitope structure is proposed to contain a trisulfated disaccharide, [-IdoA(2-OSO_3)-$GlcNSO_3$(6-OSO_3)-], which supports HS binding to various macromolecules such as growth factors and cytokines in central nervous tissues. Chemically modified heparins that lack the trisulfated disaccharides failed to inhibit the RB4CD12 recognition of HS chains. To determine the localization of the RB4CD12 anti-HS epitope in the brain, we performed an immunohistochemical analysis for cryo-cut sections of mouse brain. The RB4CD12 staining signals were colocalized with laminin and abundantly detected in the vascular basement membrane. Bacterial heparinases eliminated the RB4CD12 staining signals. The RB4CD12 epitope localization was confirmed by immunoelectron microscopy. Western blotting analysis revealed that the size of a major RB4CD12-positive molecule is ~ 460 kDa in a vessel-enriched fraction of the mouse brain. Disaccharide analysis with reversed-phase ion-pair HPLC showed that [-IdoA(2-OSO_3)-$GlcNSO_3$(6-OSO_3)-] trisulfated disaccharide residues are present in HS purified from the vessel-enriched brain fraction. These results indicated that the RB4CD12 anti-HS epitope exists in large quantities in the brain vascular basement membrane.

Keywords: basement membrane/brain vessels/heparan sulfate/HPLC/scFv antibody

INTRODUCTION

Heparan sulfate proteoglycans (HSPGs) are found on the cell surface and in the extracellular matrix, and they consist of core protein to which one or more heparan sulfate (HS) chains are covalently bound (Bernfield et al. 1999; Esko and Lindahl 2001). HS chains and heparins, structural analogues of HS chains, are members of the family of

glycosaminoglycans comprised of repeating disaccharide units of glucuronic/iduronic acid (GlcA/IdoA) and glucosamine (GlcN), which are modified through a set of deacetylation, epimerization, and sulfation reactions (Gallagher 2001). The *N*-, 3-*O*, and 6-*O* positions of GlcN and the 2-*O* position of the uronic acid residues in the disaccharide units are potentially substituted by sulfate groups by a series of Golgi-resident HS sulfotransferases (Habuchi et al. 2004). These synthetic reactions along the HS chains are spatially and temporally regulated, conferring upon the chains structural diversity, which underlies important roles in pathological and biological processes (Bishop et al. 2007; Nakato and Kimata 2002; Parish 2006; Yan and Lin 2009). HS contains highly sulfated domains and partially sulfated or non-sulfated domains, which are transitional (Gallagher 2001). Highly sulfated domains are the most common units in heparin. Within the domains, a trisulfated disaccharide structure [-IdoA(2-OSO_3)-GlcNSO_3(6-OSO_3)-] is present. This structure is considered to be a key element in molecular interactions between HS/heparin and many ligands, including growth factors, chemokines, morphogens, and lipoproteins (Bernfield et al. 1999; Esko and Selleck 2002). The trisulfated disaccharides of heparin (Morimoto-Tomita et al. 2005; Saad et al. 2005) and heparan sulfate (Ai et al. 2003; Lamanna et al. 2008; Viviano et al. 2004) are degraded by endoglucosamine 6-sulfatases, Sulf-1 and Sulf-2, in the extracellular space. The Sulfs are thought to reverse the association between angiogenic factors and heparin/HSPGs (Morimoto-Tomita et al. 2005; Uchimura et al. 2006).

Vessels in the brain are essential for functions of blood-brain barriers as well as CNS angiogenesis (Risau and Wolburg 1990). The brain vasculature is also considered to be a niche that conditions brain stem cells for further lineaging (Palmer et al. 2000). Molecules of the basement membrane of brain vasculature include HSPGs and laminin. The basement membrane HSPGs can function as both pro- and anti-signaling molecules. They can stimulate cell signaling by binding to and concentrating growth factors through their HS chains in close proximity to cell-surface receptors. On the other hand, basement membrane HSPGs can reduce signaling by sequestering growth factors away from their receptors. Regulation is achieved by the balance of inhibitory versus stimulatory forms of HS, which is ultimately controlled by the specific sulfation modifications on the HS chains (Gallagher 2001).

To evaluate the expression and localization of the specific sulfation modifications of HS in cultures and tissues, antibodies against HS have been established as useful tools (van den Born et al. 2005). The HS epitopes of recently developed phage display antibodies have been defined using derivatives of HS and heparins (van Kuppevelt et al. 1998). One of them, RB4CD12, recognizes *N*- and *O*-sulfated saccharides of HS/heparin (Dennissen et al. 2002; Jenniskens et al. 2000). The *N*-, 2-*O*, and 6-*O* sulfation, and C-5 epimerization of HS are important determinants for the antibody recognition. Its recognition epitope is proposed to be a trisulfated disaccharide-containing HS oligosaccharide (Jenniskens et al. 2002). We have shown that the RB4CD12 epitope is degraded by Sulfs *in vitro* and *ex vivo* and that the antibody can be utilized to measure the activity of the Sulfs (Hossain et al. 2010; Lemjabbar-Alaoui et al. 2010; Uchimura et al. 2010). Here we describe the RB4CD12 anti-HS epitope abundant in the brain vascular basement membrane and structural analysis of HS chains in brain vessel-enriched fractions.

MATERIALS AND METHODS

Materials

The RB4CD12 phage display-derived anti-heparan sulfate antibody (also known as HS3A8) was produced as a VSV (vesicular stomatitis virus)-tag version and purified as described previously (Dennissen et al. 2002). The following materials were obtained commercially from the sources indicated. Heparin conjugated with bovine serum albumin (Heparin-BSA), heparinases (I, II, and III), polyclonal rabbit anti-laminin antibody (Ab), monoclonal anti-VSV glycoprotein-Cy™3 Ab, monoclonal anti-FLAG® Ab, and biotinylated WFA lectin were from Sigma (St. Louis, MO); *N*-desulfated, 2-*O*-desulfated, and 6-*O*-desulfated heparins were from Neoparin Inc. (Alameda, CA); polyclonal rabbit anti-VSV-G

Ab was from Bethyl Laboratories (Montgomery, TX); alkaline phosphatase-conjugated polyclonal goat anti-rabbit IgG (H+L), Cy™2-conjugated goat anti-mouse IgG (H+L), and Cy™2-conjugated goat anti-rabbit IgG (H+L) were from Jackson Immuno Research Laboratories (West Grove, PA); biotinylated swine anti-goat IgG (H+L) and streptavidin conjugated with alkaline phosphatase were from Caltag Laboratories (Burlingame, CA); mouse anti-NeuN Ab was from Millipore (Billerica, MA); rabbit anti-Iba1 Ab was from Wako Pure Chemical Industries, Ltd. (Osaka, Japan); rabbit anti-GFAP Ab was from Thermo Scientific (Rockford, IL); mouse anti-CNPase Ab was from Abcam (Cambridge, MA); chondroitinase ABC, keratanase I, hyaluronidase, chondroitin, and chondroitin sulfate C were from Seikagaku (Tokyo, Japan); polyclonal goat anti-rabbit IgG Nanogold, ϕ1.4 nm was from Nanoprobes (Yaphank, NY); and horseradish peroxidase-conjugated goat anti-rabbit IgG was from Cell Signaling Technology, Inc. (Beverly, MA).

Animals

C57BL/6 mice were from Japan SLC Inc. (Hamamatsu, Japan). Mice were maintained in barrier facilities. The National Center of Geriatrics and Gerontology Institutional Animal Care and Use Committee approved the animal studies.

ELISA for RB4CD12 recognition

To immobilize heparin, 100 ng/ml heparin-BSA in PBS was added to the wells (100 µl/well) of a 96-well plate (Immulon 2HB, Dynex Laboratories). The plate was kept at 4°C overnight. The wells were washed 3 times with PBS containing 0.1% Tween-20 (PBS-T) and then blocked with 3% BSA (Sigma) in PBS containing 0.01% NaN_3 at room temperature (RT) for 2 h. The wells were washed as above and incubated with 100 µl/well RB4CD12 (1:750 diluted by 0.1% BSA in PBS) mixed with intact heparins, chemically modified heparins, chondroitin sulfates, or heparinase-treated heparins at RT for 1 h. The wells were washed as above and incubated with 100 µl/well secondary rabbit anti-VSV antibody (1 µg/ml in 0.1% BSA in PBS) at RT for 45 min. Then, the wells were washed and incubated with 100 µl/well of alkaline phosphatase-conjugated goat anti-rabbit IgG (0.3 µg/ml in 0.1% BSA in PBS) at RT for 45 min. The wells were washed as above and incubated with p-nitrophenyl phosphate (PNPP) (Pierce) at RT for 5 to 10 min. OD 405 nm was read on a microplate reader (Bio-Rad).

Fractionation of brain samples

A snap-frozen mouse cortex (~ 25 mg) was placed in a tube containing 600 µL (30 vol of the tissue weight) of ice-cold TBS (20 mM Tris and 137 mM NaCl, pH 7.6) and protease inhibitors (complete protease inhibitor cocktail; Roche Diagnostics). The tube was placed in a water bath of the Bioruptor ultrasonic vibration (CosmoBio, Tokyo). The tissue was fragmented by sonicating the tube for 15 sec with the maximum ultrasonic wave output power 4 to 5 times until solid materials in the tube became invisible. The material was ultracentrifuged at 100,000 x g for 20 min at 4°C. The supernatant was collected and stored frozen as "TBS soluble fraction". The resulting precipitate was suspended in 600 µL (the same volume as above) of TBS containing 1% SDS. The suspension was centrifuged at 12,000 rpm for 20 min at RT. The resulting supernatant was collected and stored frozen as "SDS soluble fraction". The protein concentrations of both fractions were measured with a BCA Protein Assay Reagent Kit (Thermo Scientific). Twenty-five mg of frozen mouse brain cortex was placed on a glass Petri dish and minced with a blade. The tissues were transferred into a tube containing 1 ml of ice-cold TBS. The tissues were homogenized with a Dounce homogenizer. The homogenate was filtered with a 100 µm nylon mesh. The filtered materials were collected and then applied to a 40 µm nylon mesh. Residues on the filters were suspended in 100 µL of TBS containing 1% SDS ("vessel-enriched fraction"). Materials filtered through the 40 µm nylon mesh were collected and mixed with the same volume of TBS containing 2% SDS ("flow-through fraction"). Methylene blue staining and bright field microscopy confirmed cerebral blood vessels on the filters.

Immunohistochemistry

Fresh brains from 12-week-old C57BL/6 mice were embedded in the O.C.T. compound (Sakura Finetek, Torrance, CA) and frozen in liquid nitrogen. The brains were stored at -80°C until analysis. Cryostat-cut sections (10 μm thick) were prepared on MAS-coated glass slides (Matsunami, Osaka, Japan), fixed in ice-cold acetone for 15 min, and then air-dried for 30 min. Sections were incubated with blocking solution (3% BSA in PBS) for 15 min at RT. Sections were washed twice with PBS and then incubated with a mixture of RB4CD12 (1:100 dilution) and rabbit anti-laminin antibody (1:100 dilution, Sigma) for 1 h at RT. Then, primary antibodies were detected with Cy3-conjugated monoclonal anti-VSV-G (4 μg/ml) and Cy2-conjugated polyclonal goat anti-rabbit IgG (3 μg/ml). Sections were mounted in FluorSave™ Reagent (Merck, Darmstadt, Germany). Digital images were captured by fluorescent microscopy (model BX50, Olympus) at the same setting for all images. To determine the effects of GAG degrading enzymes, 3% BSA-blocked sections were pre-treated with 100 μL of a reaction mixture containing 5 μmol of HEPES, pH 7.5, and enzymes (a mixture of 1 mU heparinase I, 0.25 mU heparinase II, and 0.1 mU heparinase III, 50 mU chondroitinase ABC, 250 mU keratanase I, or 250 mTRU hyaluronidase) at 37 °C overnight. For pretreatment with the mixture of heparitinases, 1 μmol of $MgCl_2$ was added to the reaction mixture.

Immunoelectron microscopy
Cryostat-cut sections from 12-week-old C57BL/6 mouse brain were prepared on MAS-coated glass slides, fixed in 4% paraformaldehyde for 5 min, then washed with PBS for 1 h. Sections were incubated with 3% BSA for 30 min at RT. Diluted RB4CD12 antibody (1:40) was then applied overnight. After washing, diluted rabbit anti-VSV secondary (7.2 μg/ml) was applied for 1 h. After several washes, diluted goat anti-rabbit IgG antibody coupled with 1.4-nm-diameter tertiary gold particles (1:40) was applied for 30 min. The samples were then washed and fixed in 2% glutaraldehyde in 0.1 M sodium cacodylate buffer (pH 7.4) for 3 h, followed by enlargement of the gold particles with an HQ-Silver Enhancement Kit (Nanoprobes). The specimens were examined in a Hitachi H-7600 transmission electron microscope (Tokyo, Japan).

Immunoblots
The proteins (40 μg per lane) were separated by NuPAGE 3-8% polyacrylamide gel electrophoresis (Invitrogen), and blotted onto a PVDF membrane (Millipore). The membrane was blocked with 5% skim milk /PBS-T for 1 h at room temperature and then incubated overnight with RB4CD12 antibody (1:500) in TBS-T at 4°C. The membrane was washed and incubated with horseradish peroxidase-conjugated mouse anti-VSV (1:2000) for 1 h at RT. Bound antibodies were visualized with SuperSignal West Dura Chemiluminescent reagent (Thermo Scientific). Signals were visualized and quantified using a LAS-3000 mini luminescent image analyzer (Fujifilm, Tokyo, Japan).

Preparation and structural analysis of HS
Two hundred and fifty mg of frozen mouse cortex or the cortical vessel residue that remained on filters described above was suspended in 2 mL of 0.2N NaOH and incubated overnight at RT. The samples were neutralized with 4N HCl and then treated with DNase I and RNase A (0.04 mg/ml each) (Roche) in 50 mM Tris-HCl, pH8.0, 10 mM $MgCl_2$ for 3 h at 37°C. Subsequently, the samples were treated with actinase E (0.04 mg/ml) (Kaken Pharmaceutical Co., Ltd., Tokyo, Japan) overnight at 37°C. The supernatant was collected by centrifugation at 5,000 x g at 4°C for 10 min after heat inactivation of the enzyme and then mixed with the same volume of 50 mM Tris-HCl, pH 7.2. The HS was purified by DEAE-Sepharose column chromatography as reported previously (Habuchi et al. 2007). The disaccharide compositions of the HS were determined by reversed-phase ion-pair chromatography with post-column fluorescent labeling adapted from a method in a previous report (Toyoda et al. 2000). The level of total HS was determined by summing amounts of all disaccharides detected in each sample. All data are presented as means ± S.D. unless noted otherwise. The values were analyzed by Prism software (GraphPad Software, La Jolla, CA).

RESULTS

Modified heparins that lack trisulfated disaccharide units do not interfere with the RB4CD12 recognition

RB4CD12 is a single-chain variable fragment (scFv) antibody selected for reactivity to skeletal muscle heparin/HS glycosaminoglycans utilizing a phage display system (Jenniskens et al. 2000). Antibody binding depends on all three sulfate modifications (Dennissen et al. 2002). To further characterize the RB4CD12 recognition determinants, we performed a cell-free ELISA with chemically modified heparins. The RB4CD12 antibody recognized heparin-BSA (10 ng) immobilized onto plastic wells (Fig. 1). RB4CD12 binding to heparin-BSA was substantially reduced by pre-mixing with an intact heparin in a dose-dependent manner. Chemically modified heparins that are 2-*O*-desulfated or 6-*O*-desulfated showed much less inhibition even at higher concentrations (Fig. 1A), suggesting that the RB4CD12 antibody is highly specific to a trisulfated disaccharide-containing HS oligosaccharide. *N*-desulfated heparin, chondroitin, and chondroitin 6-sulfate (CS-C) did not affect the RB4CD12 recognition. Pre-treatment of the heparin-BSA with a mixture of heparitinases eliminated the RB4CD12 recognition (Fig. 1B).

The RB4CD12 epitope is abundant in the basement membrane of vessels in the brain

Previous study has shown that different HS epitopes should have a defined distribution and be tightly, topologically regulated (Dennissen et al. 2002). To determine whether expression of the trisulfated disaccharide-containing HS is spatially regulated in the brain, we immunohistochemically analyzed the distribution of the RB4CD12 epitope in the brain. Cryostat-cut sections of C57BL/6 mouse brains were immunostained with the RB4CD12 antibody and each cell type-specific antibody. As shown in Fig. 2, RB4CD12 staining signals clearly colocalized with laminin, which is abundant in the basement membrane of vessels and used as a marker for brain vasculature (Laurie et al. 1982). GFAP, a marker for astrocytes, partly colocalized with the RB4CD12 staining signals at the gliovascular interface (Fig. 2, arrowheads). The RB4CD12 epitope was hardly detected in cells that are positive for NeuN, a marker for neurons. Neither IbaI, a marker for microglia, nor CNPase, a marker for oligodendrocytes, was immunolocalized with the RB4CD12 staining signals (Fig. 2). WFA lectin, which is often used as a marker for perineuronal nets that are rich in chondroitin sulfates, did not colocalize with the RB4CD12 signals (Fig. 2). Similar results were also observed in the hippocampus and cerebellum (not shown). These results indicated that the RB4CD12 epitope exists in large quantities in the basement membrane of brain vessels. To confirm that the observed signals in Fig. 2 arose from a trisulfated disaccharide-containing HS oligosaccharide, we pre-treated brain sections with a mixture of heparinases, chondroitinase ABC, karatanase I, or hyaluronidase, and then stained with the RB4CD12 antibody and an anti-laminin antibody. Only treatment with a mixture of heparinases eliminated RB4CD12 immunoreactivity (Fig. 3). To determine the ultrastructural localization of the RB4CD12 epitope in the basement membrane of the brain vessels, we carried out immunoelectron microscopy. Cryostat-cut sections from C57BL/6 mouse brains were immunostained with the RB4CD12 antibody followed by probing with a rabbit anti-VSV secondary antibody and a goat anti-rabbit IgG tertiary antibody conjugated with gold particles. After enlargement of the gold particles, the specimens were embedded in water miscible epoxy resins and examined under a transmission electron microscope. We observed that most RB4CD12 immunogold particles were present in the area of the basement membrane of cerebral vessels (Fig. 4, right panel, arrowheads).

The RB4CD12 epitope is dominantly borne on molecules of 460 kDa in vessel-enriched fractions

Next, we prepared vessel-enriched fractions of mouse cortices and examined the immunoreactivity of the RB4CD12 antibody. Immunoblotting with the anti-laminin antibody indicated that the vessel-enriched fraction was properly fractionated (Fig. 5, lower panel). A band with a molecular weight of ~ 460 kDa was

dominant in an immunoblot with the RB4CD12 antibody in the vessel-enriched fractions (Fig. 5).

Trisulfated disaccharides of heparan sulfate are detected in vessel-enriched fractions

Finally, we carried out structural analysis of HS chains in the vessel-enriched fractions of mouse brain. HS was isolated from the whole cortex and the cortical vessel-enriched fractions of adult mice and depolymerized into its constituent disaccharides by a mixture of bacterial heparitinases. The disaccharide compositions of the HS were determined by reversed-phase ion-pair chromatography. We found that 2.3% of the total disaccharides were trisulfated disaccharides in the vessel-enriched fractions. The presence of the trisulfated disaccharides was consistent with the fact that RB4CD12 recognizes the vessels in the brain. The content of total HS in the vessel-enriched fractions of the adult mouse cortex was 5% of that in the whole cortex fraction (Fig. 6).

DISCUSSION

In the present study, we found that the immunoreactivity of the RB4CD12 antibody was colocalized with the laminin immunoreactivity, suggesting that the RB4CD12 epitope is largely present in the basement membrane of vessels in the brain. The immunoelectron microscopy analysis confirmed the localization of the RB4CD12 epitope in the vascular basement membrane. These findings are correlated with those of a previous report that demonstrated that RB4CD12 stains the skeletal muscle basal lamina (Jenniskens et al. 2000). We also found that the RB4CD12-positive ~460 kDa band was present in the immunoblot of the vessel-enriched fractions. Perlecan, agrin, and type XVIII collagen are the major HSPGs present in the basement membrane of the brain vasculature (Bezakova and Ruegg 2003; Iozzo 2005). The size of core protein of perlecan is known to be ~ 460 kDa. It can reach a molecular weight of over 800 kDa together with HS chains. Agrin has a 225 kDa core protein and its glycosylation modifications increase the molecular weight to ~ 500 kDa in the brain (Donahue et al. 1999). Type XVIII collagen shows molecular weights ~ 200 kDa (Elamaa et al. 2003). Our results in Western blotting suggest that the observed immunoreactivity of the RB4CD12 antibody in the cortex might arise from the HS chains of perlecan and/or agrin. Further investigation is needed for identification of the core proteins that bear the RB4CD12 epitope expressed in the brain vasculature.

In conjunction with the RB4CD12 immunoreactivity in the laminin-positive basement membrane and vessel-enriched fractions, the disaccharide analysis showed that trisulfated disaccharides are components of HS chains in the vessel-enriched fractions. Although the percentage of trisulfated disaccharides is not substantial, it is possible that these disaccharides are clustered and form highly sulfated domains that are RB4CD12 recognition determinants within the chains. Since the recognition epitope of RB4CD12 is proposed to be [-GlcNSO$_3$(6-OSO$_3$)-IdoA(2-OSO$_3$)-GlcNSO$_3$(6-OSO$_3$)-] (Jenniskens et al. 2002), the cluster size might be two or more consecutive trisulfated disaccharides. It has been known that *N*-sulfation of GlcN residues is the initial HS sulfation and that *N*-sulfated domains are primary sites for further modification (Carlsson et al. 2008). It seems probable that *N*-sulfation could occur densely, not sparsely, in the brain vasculature, leading to the formation of trisulfated disaccharide clusters within HS polysaccharides. Expression profiles of HS sulfotransferases and sulfatases in brain vessels may provide approaches that are pertinent to understanding the mechanisms underlying the formation of the HS subdomains.

Sulf-1 and Sulf-2 are known to remove 6-*O* sulfates on glucosamine residues in the trisulfated disaccharides of HS and heparin (Ai et al. 2003; Morimoto-Tomita et al. 2002; Saad et al. 2005; Viviano et al. 2004). Sulf-2 mobilizes heparin-bound vascular endothelial growth factor (VEGF), fibroblast growth factor (FGF)-1, and stromal cell-derived factor (SDF)-1/CXCL12 (Uchimura et al. 2006). Our previous study has shown that treatment of mouse brain sections with Sulf-1 or Sulf-2 diminished the immunoreactivity of RB4CD12 in the brain vessels *ex vivo* (Hossain et al. 2010). Considering the results of the present study, the RB4CD12-positive HS subdomains might be important for supporting interactions between

the HS chains and macromolecules such as growth factors in the basement membrane of the brain vessels. Increasing evidence has shown that highly sulfated domains within HS chains of HSPGs support the interaction with HS-binding factors. VEGF binds to perlecan (Jiang and Couchman 2003). HSPGs could act as storage sites of VEGF in the vessel wall. The release of growth factors from the complex with HSPGs through proteolytic processing and HS degradation is a physiological mechanism that disengages biologically active molecules from its storage site (Bergers et al. 2000; Iozzo 1998). In the basement membrane of vessels, VEGF is stored by binding to HSPGs and could be released by the action of Sulfs to exert proangiogenic activity (Morimoto-Tomita et al. 2005; Uchimura et al. 2006). Our results describing the abundance of the RB4CD12 epitope in the basement membrane of the brain vessels could emphasize the roles of the trisulfated disaccharide-containing HS domains in the storage and release of HS-bound growth factors, especially VEGF. Furthermore, endothelial cells bind to the perlecan protein core (Hayashi et al. 1992), which is modulated by the presence of glycosaminoglycan chains. Our results also highlight a possible role of the RB4CD12 epitope in migration and growth of endothelial cells in the brain vasculature. Within an angiogenic niche, adult neurogenesis has been shown to occur (Palmer et al. 2000). Growth factors that are bound to the RB4CD12-positive HS subdomains might be involved in defining the neurogenic microenvironment. Future efforts to investigate the biological roles of the RB4CD12 epitope and the Sulfs in brain vessels will provide essential information on the contribution of the trisulfated disaccharide-containing HS domains to cerebrovascular angiogenesis and neurogenesis.

Acknowledgements:
We thank Steven Rosen and Tony Wyss-Coray for their helpful suggestions and discussion. We are grateful to Kuniko Takanose for technical assistance. T.H-F. is a Research Fellow of the Japan Foundation for Aging and Health.

Abbreviations used: CS, chondroitin sulfate; ECM, extracellular matrix; ELISA, enzyme-linked immunosorbent assay; HS, heparan sulfate; HSPG, heparan sulfate proteoglycan; kDa, kilodalton; PBS-T, 0.1% Tween 20 in PBS; scFv, single-chain variable fragment.

REFERENCES

Ai X, Do AT, Lozynska O, Kusche-Gullberg M, Lindahl U, Emerson CP, Jr. 2003. QSulf1 remodels the 6-O sulfation states of cell surface heparan sulfate proteoglycans to promote Wnt signaling. J Cell Biol 162:341-351.

Bergers G, Brekken R, McMahon G, Vu TH, Itoh T, Tamaki K, Tanzawa K, Thorpe P, Itohara S, Werb Z, Hanahan D. 2000. Matrix metalloproteinase-9 triggers the angiogenic switch during carcinogenesis. Nat Cell Biol 2:737-744.

Bernfield M, Gotte M, Park PW, Reizes O, Fitzgerald ML, Lincecum J, Zako M. 1999. Functions of cell surface heparan sulfate proteoglycans. Annu Rev Biochem 68:729-777.

Bezakova G, Ruegg MA. 2003. New insights into the roles of agrin. Nat Rev Mol Cell Biol 4:295-308.

Bishop JR, Schuksz M, Esko JD. 2007. Heparan sulphate proteoglycans fine-tune mammalian physiology. Nature 446:1030-1037.

Carlsson P, Presto J, Spillmann D, Lindahl U, Kjellen L. 2008. Heparin/heparan sulfate biosynthesis: processive formation of N-sulfated domains. J Biol Chem 283:20008-20014.

Dennissen MA, Jenniskens GJ, Pieffers M, Versteeg EM, Petitou M, Veerkamp JH, van Kuppevelt TH. 2002. Large, tissue-regulated domain diversity of heparan sulfates demonstrated by phage display antibodies. J Biol Chem 277:10982-10986.

Donahue JE, Berzin TM, Rafii MS, Glass DJ, Yancopoulos GD, Fallon JR, Stopa EG. 1999. Agrin in Alzheimer's disease: altered

solubility and abnormal distribution within microvasculature and brain parenchyma. Proc Natl Acad Sci U S A 96:6468-6472.

Elamaa H, Snellman A, Rehn M, Autio-Harmainen H, Pihlajaniemi T. 2003. Characterization of the human type XVIII collagen gene and proteolytic processing and tissue location of the variant containing a frizzled motif. Matrix Biol 22:427-442.

Esko JD, Lindahl U. 2001. Molecular diversity of heparan sulfate. J Clin Invest 108:169-173.

Esko JD, Selleck SB. 2002. Order out of chaos: assembly of ligand binding sites in heparan sulfate. Annu Rev Biochem 71:435-471.

Gallagher JT. 2001. Heparan sulfate: growth control with a restricted sequence menu. J Clin Invest 108:357-361.

Habuchi H, Habuchi O, Kimata K. 2004. Sulfation pattern in glycosaminoglycan: does it have a code? Glycoconj J 21:47-52.

Habuchi H, Nagai N, Sugaya N, Atsumi F, Stevens RL, Kimata K. 2007. Mice deficient in heparan sulfate 6-O-sulfotransferase-1 exhibit defective heparan sulfate biosynthesis, abnormal placentation, and late embryonic lethality. J Biol Chem 282:15578-15588.

Hayashi K, Madri JA, Yurchenco PD. 1992. Endothelial cells interact with the core protein of basement membrane perlecan through beta 1 and beta 3 integrins: an adhesion modulated by glycosaminoglycan. J Cell Biol 119:945-959.

Hossain MM, Hosono-Fukao T, Tang R, Sugaya N, van Kuppevelt TH, Jenniskens GJ, Kimata K, Rosen SD, Uchimura K. 2010. Direct detection of HSulf-1 and HSulf-2 activities on extracellular heparan sulfate and their inhibition by PI-88. Glycobiology 20:175-186.

Iozzo RV. 1998. Matrix proteoglycans: from molecular design to cellular function. Annu Rev Biochem 67:609-652.

Iozzo RV. 2005. Basement membrane proteoglycans: from cellar to ceiling. Nat Rev Mol Cell Biol 6:646-656.

Jenniskens GJ, Hafmans T, Veerkamp JH, van Kuppevelt TH. 2002. Spatiotemporal distribution of heparan sulfate epitopes during myogenesis and synaptogenesis: a study in developing mouse intercostal muscle. Dev Dyn 225:70-79.

Jenniskens GJ, Oosterhof A, Brandwijk R, Veerkamp JH, van Kuppevelt TH. 2000. Heparan sulfate heterogeneity in skeletal muscle basal lamina: demonstration by phage display-derived antibodies. J Neurosci 20:4099-4111.

Jiang X, Couchman JR. 2003. Perlecan and tumor angiogenesis. J Histochem Cytochem 51:1393-1410.

Lamanna WC, Frese MA, Balleininger M, Dierks T. 2008. Sulf loss influences N-, 2-O-, and 6-O-sulfation of multiple heparan sulfate proteoglycans and modulates fibroblast growth factor signaling. J Biol Chem 283:27724-27735.

Laurie GW, Leblond CP, Martin GR. 1982. Localization of type IV collagen, laminin, heparan sulfate proteoglycan, and fibronectin to the basal lamina of basement membranes. J Cell Biol 95:340-344.

Lemjabbar-Alaoui H, van Zante A, Singer MS, Xue Q, Wang YQ, Tsay D, He B, Jablons DM, Rosen SD. 2010. Sulf-2, a heparan sulfate endosulfatase, promotes human lung carcinogenesis. Oncogene 29:635-646.

Morimoto-Tomita M, Uchimura K, Bistrup A, Lum DH, Egeblad M, Boudreau N, Werb Z, Rosen SD. 2005. Sulf-2, a proangiogenic heparan sulfate endosulfatase, is upregulated in breast cancer. Neoplasia 7:1001-1010.

Morimoto-Tomita M, Uchimura K, Werb Z, Hemmerich S, Rosen SD. 2002. Cloning and characterization of two extracellular heparin-degrading endosulfatases in mice and humans. J Biol Chem 277:49175-49185.

Nakato H, Kimata K. 2002. Heparan sulfate fine structure and specificity of proteoglycan functions. Biochim Biophys Acta 1573:312-318.

Palmer TD, Willhoite AR, Gage FH. 2000. Vascular niche for adult hippocampal neurogenesis. J Comp Neurol 425:479-494.

Parish CR. 2006. The role of heparan sulphate in inflammation. Nature reviews 6:633-643.

Risau W, Wolburg H. 1990. Development of the blood-brain barrier. Trends Neurosci 13:174-178.

Saad OM, Ebel H, Uchimura K, Rosen SD, Bertozzi CR, Leary JA. 2005. Compositional profiling of heparin/heparan sulfate using mass spectrometry: Assay for specificity of a novel extracellular human endosulfatase. Glycobiology.

Toyoda H, Kinoshita-Toyoda A, Selleck SB. 2000. Structural analysis of glycosaminoglycans in Drosophila and Caenorhabditis elegans and demonstration that tout-velu, a Drosophila gene related to EXT tumor suppressors, affects heparan sulfate in vivo. J Biol Chem 275:2269-2275.

Uchimura K, Lemjabbar-Alaoui H, van Kuppevelt TH, Rosen SD. 2010. Use of a phage display antibody to measure the enzymatic activity of the Sulfs. Methods Enzymol 480:51-64.

Uchimura K, Morimoto-Tomita M, Bistrup A, Li J, Lyon M, Gallagher J, Werb Z, Rosen SD. 2006. HSulf-2, an extracellular endoglucosamine-6-sulfatase, selectively mobilizes heparin-bound growth factors and chemokines: effects on VEGF, FGF-1, and SDF-1. BMC Biochem 7:2.

van den Born J, Salmivirta K, Henttinen T, Ostman N, Ishimaru T, Miyaura S, Yoshida K, Salmivirta M. 2005. Novel heparan sulfate structures revealed by monoclonal antibodies. The Journal of biological chemistry 280:20516-20523.

van Kuppevelt TH, Dennissen MA, van Venrooij WJ, Hoet RM, Veerkamp JH. 1998. Generation and application of type-specific anti-heparan sulfate antibodies using phage display technology. Further evidence for heparan sulfate heterogeneity in the kidney. J Biol Chem 273:12960-12966.

Viviano BL, Paine-Saunders S, Gasiunas N, Gallagher J, Saunders S. 2004. Domain-specific modification of heparan sulfate by Qsulf1 modulates the binding of the bone morphogenetic protein antagonist Noggin. J Biol Chem 279:5604-5611.

Yan D, Lin X. 2009. Shaping morphogen gradients by proteoglycans. Cold Spring Harb Perspect Biol 1:a002493.

LEGENDS TO FIGURES

Figure 1. Inhibition ELISA for the RB4CD12 recognition determinant
(A). Binding of the RB4CD12 antibody to heparin-BSA coated on plates was measured in the presence of heparin, chemically modified heparin, or chondroitin sulfate shown on the right. (B). The binding of RB4CD12 in the presence of heparin that was pre-treated with a mixture of heparinase I, heparinase II, and heparinase III was measured. Hep-de2S, 2-*O*-desulfated heparin; Hep-de6S, 6-*O*-desulfated heparin; Hep-deNS, *N*-desulfated heparin; CS-C, chondroitin 6-sulfate; Ch, chondroitin.

Figure 2. Immunoreactivity of RB4CD12 is colocalized with laminin in the mouse brain
RB4CD12 binding was visualized using a Cy3-conjugated anti-VSV tag antibody with fluorescence microscopy (*red*). Basement membrane of brain vasculature and different types of cells were co-stained by cell type-specific antibodies, laminin, NeuN, CNPase, GFAP, Iba1, or biotinylated WFA lectin in conjunction with Cy2-conjugated secondary antibodies or streptavidin (*green*). RB4CD12 staining signals were colocalized with laminin staining in the basement membrane of brain vessels (*arrowheads*). GFAP partly colocalized with the RB4CD12 signals at the interface between vessels and astrocytes (*arrows*). Bar denotes 50 μm.

Figure 3. Immunoreactivity of RB4CD12 is eliminated by pre-treatment of brain sections with heparinases
Cryostat-cut sections of mouse brains were pre-incubated overnight with glyosaminoglycan-degrading enzymes. RB4CD12 binding was visualized using a Cy3-conjugated anti-VSV tag antibody with fluorescence microscopy (*red*). Basement membranes of vessels were co-stained using an anti-laminin antibody in conjunction with a Cy2-conjugated secondary antibody (*green*). RB4CD12 signals in the microvasculature basement membrane of vessels were eliminated by a mixture of heparinase I, heparinase II, and heparinase III (Heparinases). Chase ABC, chondroitinase ABC. Bar denotes 50 μm.

Figure 4. Immunoelectron microscopy for the RB4CD12 epitope in the mouse brain
Low magnification (*left*) and high magnification (*right*) scanning electron micrographs are shown. RB4CD12 immunogold particles, singularly or in clusters, decorate electron-lucid layers in the basement membrane (BM) of a vessel indicated by arrowheads. N, nucleus; L, vessel lumen.

Figure 5. Immunoblotting analysis of the RB4CD12 epitope in vessel-enriched fractions of the mouse cortex
Immunoblot with RB4CD12 and anti-laminin antibodies for vessel-enriched fractions of the mouse cortex. Lane 1, vessel-enriched fraction; lane 2, flow-through fraction; lane 3 whole cortex fraction.

Figure 6. Disaccharide analysis of heparan sulfate in vessel-enriched fractions of the mouse cortex
Heparan sulfates were purified from whole tissues (whole) or vessel-enriched fractions (vessels fr) of mouse cerebral cortices, and then degraded with a mixture of heparinases I, II, and III. The produced disaccharides were analyzed by post-labeling reversed-phase ion-pair HPLC. The values are representative of two independent experiments.

Figure 1

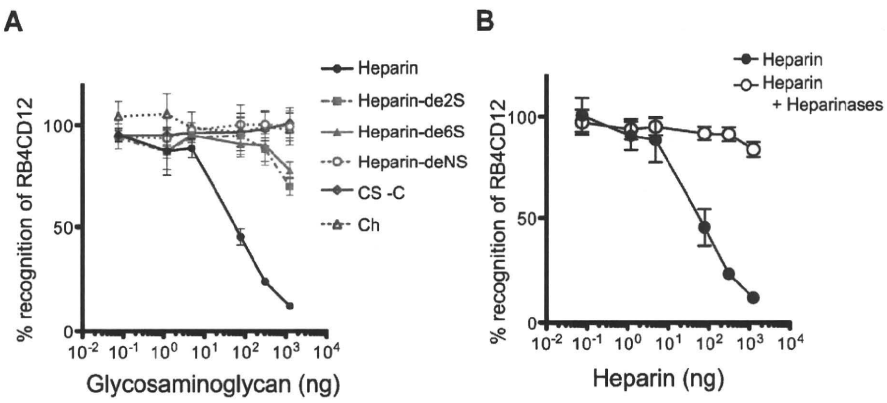

188x166mm (600 x 600 DPI)

Figure 2

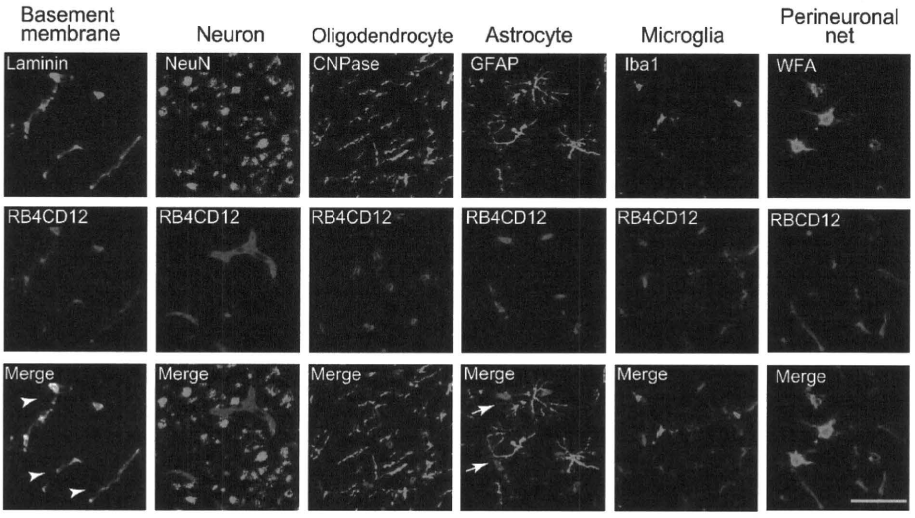

234x159mm (600 x 600 DPI)